Journal of Solid State Chemistry **156,** 68–74 (2001)
doi:10.1006/jssc.2000.8964, available online at http://www.idealibrary.com on IDEAL®

Praseodymium Deficiency Effects on the Physical Properties of $Pr_{0.7-x}\square Sr_{0.3}MnO_3$ Perovskite Manganites

W. Boujelben[1] and A. Cheikh-Rouhou

Laboratoire de Physique des Matériaux, Faculté des Sciences de Sfax, B.P. 802, 3018 Sfax, Tunisie

and

J. C. Joubert

Laboratoire des Matériaux et du Génie Physique, ENSPG-CNRS (UMR-5628), B.P. 46, 38402 Saint Martin d'Hères Cedex, France

Received April 10, 2000; in revised form August 2, 2000; accepted September 15, 2000; published online December 21, 2000

The praseodymium deficiency effects on the structural, magnetic, and electrical properties of the lacunar perovskite manganite oxides $Pr_{0.7-x}\square_xSr_{0.3}MnO_3$ ($0 \le x \le 0.23$) have been investigated. This study is of great interest because it gives more information on the role of the Mn cation oxidation degree. Powder X-ray diffraction patterns are indexed in the rhombohedral perovskite structure with the $R\bar{3}c$ space group for $x = 0$ to 0.1 and in the orthorhombic one with the *Pbnm* space group for $x = 0.15$ to 0.23. Magnetization and resistivity measurements versus temperature show that all of our samples exhibit a semiconducting paramagnetic–metallic ferromagnetic transition when the temperature decreases. © 2001 Academic Press

Key Words: **perovskite; manganite; ferromagnetic; lacunar.**

I. INTRODUCTION

With the discovery of the large negative magnetoresistance in the perovskite manganite oxides of general formula $Ln_{1-x}M_xMnO_3$, where *Ln* is a trivalent rare-earth and *M* is a divalent alkaline-earth, interest has been focused on the study of the structural and physical properties of the related systems (1–7). The interplay between electrical transport and ferromagnetism in these systems was traditionally interpreted within the framework of a double-exchange (DE) interaction (8–10). This DE considers the magnetic coupling between Mn^{3+} and Mn^{4+} ions as resulting from the motion of an electron between two partially filled *d* shells with strong on-site Hund's coupling. However, recent studies have shown that the DE alone cannot explain the behaviors observed in these systems and suggested that other effects play a crucial role, such as charge ordering, average A-site cationic radius $\langle r_A \rangle$ (11–13), the A-site cationic size mismatch (14, 15), the oxygen deficiency (16–18), and the polaron effect due to the strong electron–phonon interaction arising from the Jahn–Teller distortion (19). These systems have been given much attention because they could possibly be used for sensor applications (20, 21), and especially to increase data storage by increasing the sensitivity of hard drive read heads (22). Due to the vast technological possibility of GMR devices, and the interest in the origin of the mechanism of this effect, a great deal of effort is being devoted to the search for materials exhibiting this important property. Thus, many studies are being performed on the transport and magnetic properties of these materials. The effects of divalent alkaline-earth elements substitution in the stoichiometric perovskite manganites $Ln_{1-x}M_xMnO_3$ have been extensively studied (11, 23–25). These studies showed that the Curie temperature T_C and the magnetoresistance effects are optimized for a Mn^{4+} content of about 30%. However, only a few studies have been done on deficiency effects in lacunar systems (26–28). Deficiencies in the perovskite A-site lead to an increase in the Mn^{4+} content. Recent studies on the strontium deficiency effects in $Pr_{0.7}Sr_{0.3-x}\square_xMnO_3$ (29) showed a structural transition from a rhombohedral to an orthorhombic system for $x > 0.2$ and a decrease in the Curie temperature T_C with increasing deficiency content. In order to study the praseodymium vacancy effects in $Pr_{0.7}Sr_{0.3}MnO_3$, we investigate the structural, magnetic, and electrical properties in the $Pr_{0.7-x}\square_xSr_{0.3}MnO_3$ lacunar system. In such systems, the divalent element content is fixed at 30%, and praseodymium vacancies imply an increase of the Mn^{4+} content beyond 30% and also a change in the average ionic radius $\langle r_A \rangle$ of the A-site.

[1]To whom correspondence should be addressed. Fax: 216 4 274 437. E-mail: Abdel.Cheikhrouhou@fss.rnu.tn.

0022-4596/01 $35.00

II. EXPERIMENTAL

Powder samples $Pr_{0.7-x}\square_xSr_{0.3}MnO_3$ $(0 \le x \le 0.23)$ are prepared by mixing Pr_6O_{11}, Mn_2O_3, and $SrCO_3$ up to 99.9% purity in the desired proportion according to the following reaction:

$$(0.7 - x)Pr_6O_{11} + 1.8SrCO_3 + 3Mn_2O_3$$

$$\rightarrow 6Pr_{0.7-x}\square_xSr_{0.3}MnO_3 + \delta CO_2.$$

The starting materials are mixed in an agate mortar and then heated in air at 1000°C for 60 hours. Systematic annealing at high temperature is necessary to ensure a complete reaction. In fact, the powders are pressed into pellets (of about 1 mm thickness) and sintered at 1400°C in air for 60 hours with intermediate regrinding and repelling. Finally these pellets are rapidly quenched in water.

Phase purity, homogeneity, and cell dimensions are determined by powder X-ray diffraction at room temperature (diffractometry using Fe radiation and Si powder as internal standard). Unit cell dimensions are obtained by least-squares calculations.

Magnetization measurements versus temperature are recorded by using a vibrating sample magnetometer in the temperature range 10–350 K, using an applied field of 500 Oe.

Resistivity measurements are performed using the conventional four-probe method in the Earth's magnetic field.

III. RESULTS AND DISCUSSION

1. X-ray Diffraction Analysis

X-ray patterns at room temperature of some samples are shown in Fig. 1. All of our samples are in a single phase; however, for high x values, we remark the presence of diffraction peaks with very small intensities, which are attributed to traces of Mn_3O_4.

Structural study shows that all of the samples have a perovskite structure with different distortion degrees.

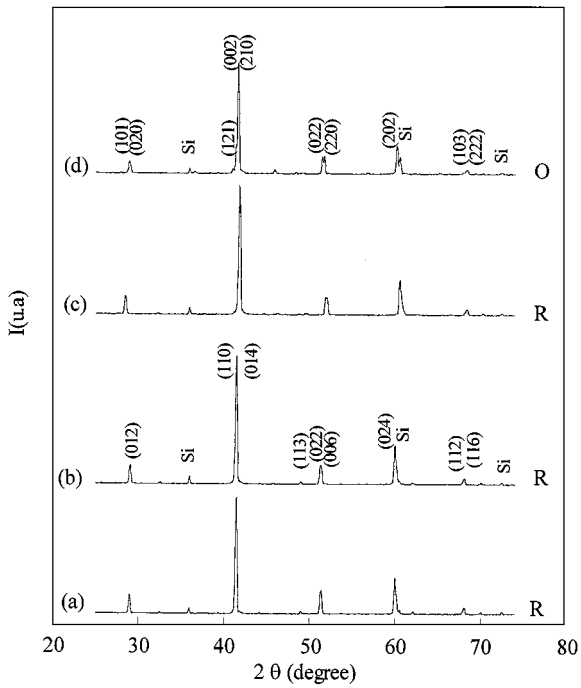

FIG. 1. X-ray diffraction powder patterns for some perovskite $Pr_{0.7-x}\square_xSr_{0.3}MnO_3$ samples. (a) $x = 0$; (b) $x = 0.05$; (c) $x = 0.1$, (d) $x = 0.2$. O, orthorhombic; R, rhombohedral.

Samples corresponding to $x = 0$ to 0.1 crystallize in a rhombohedral structure with the $R\bar{3}c$ space group, while samples with $0.15 \le x \le 0.23$ crystallize in orthorhombic symmetry with the *Pbnm* space group. Sample purity and composition were checked by both electron diffraction scanning and neutron diffraction. Neutron diffraction investigations, which confirmed the Pr deficiency and the oxygen stoichiometry in our samples, will be published elsewhere.

In Table 1, we list the lattice parameters and the unit cell volume of $Pr_{0.7-x}\square_xSr_{0.3}MnO_3$ samples. The room temperature unit cell volume (V) is systematically decreased as the vacancies content increases.

TABLE 1
Crystallographic Data for $Pr_{0.7-x}\square_xSr_{0.3}MnO_3$ Samples

x	Symmetry[a]	a_r (Å)	α_r (°)	a (Å)	b (Å)	c (Å)	V (Å^3)
0.00	R	5.468(5)	60.09(3)	—	—	—	232.15
0.05	R	5.464(7)	60.12(4)	—	—	—	231.614
0.10	R	5.461(5)	60.15(3)	—	—	—	231.342
0.15	O	—	—	5.4542(7)	5.4670(7)	7.7114(6)	229.939
0.20	O	—	—	5.4822(5)	5.443(6)	7.6944(5)	229.602
0.23	O	—	—	5.4586(3)	5.4433(4)	7.6729(3)	227.980

[a]O, orthorhombic; *R*, rhombohedral.

Praseodymium deficiency implies a conversion of Mn^{3+} to Mn^{4+} with smaller ionic radius [$r(Mn^{4+}) = 0.68$ Å and $r(Mn^{3+}) = 0.785$ Å (30)] and a change in the average ionic radius of the A-site. For electrostatic considerations, a vacancy must have an average radius $\langle r_V \rangle \neq 0$. A previous study on lacunar $Pr_{0.7}Sr_{0.3-x}\square_xMnO_3$ showed that strontium deficiency leads to a strong contraction of the unit cell (29). This result indicates that the vacancy average radius $\langle r_V \rangle$ is surely smaller than that of the Sr^{2+} ion (1.31 Å). However, this vacancy average radius $\langle r_V \rangle$ may be larger than that of the Pr^{3+} ion (1.179 Å). In fact, for a given Mn^{4+} content (60%), a strontium deficiency ($Pr_{0.7}Sr_{0.15}\square_{0.15}MnO_3$) (29) leads to smaller unit cell than a praseodymium one ($Pr_{0.6}\square_{0.1}Sr_{0.3}MnO_3$).

It is important to specify that for $x = 0.15$ the lattice parameters verify $c/\sqrt{2} < a < b$, corresponding to the O′-type structure, while for $x = 0.2$ and 0.23 these parameters verify $c/\sqrt{2} < b < a$. Such a result where a and b are found to be reversed ($a > b$) has been mentioned by Knizek *et al.* for $x \geq 0.3$ in the $Pr_{1-x}Sr_xMnO_3$ system (23), and by Dabrowski *et al.* in $La_{0.87}Sr_{0.13}MnO_3$ as a function of temperature (31). It has been also observed by Ritter *et al.* in La $MnO_{3+\delta}$ as a function of oxygen content (32).

The orthorhombic phase presents a ratio $c/a < \sqrt{2}$ characteristic of a cooperative Jahn–Teller deformation.

2. Magnetic Properties

We have plotted in Fig. 2 the magnetization evolution versus temperature with an applied field of 500 Oe for the $Pr_{0.7-x}\square_xSr_{0.3}MnO_3$ system. These curves show that all samples exhibit a paramagnetic (PM)-to-ferromagnetic (FM) transition when the temperature decreases. All of the $M(T)$ curves present an anomaly at about 60 K which can be attributed to the apparatus; in fact, we observe such an anomaly in all of our measurements.

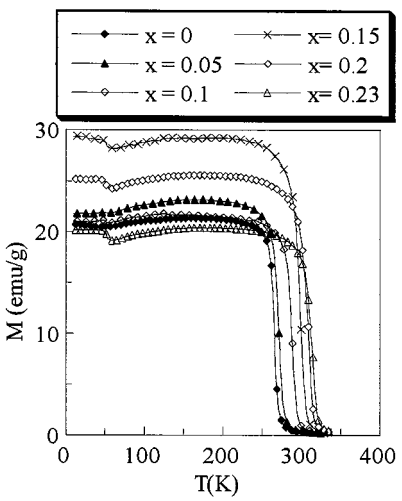

FIG. 2. Magnetization of $Pr_{0.7-x}\square_xSr_{0.3}MnO_3$ samples as a function of temperature at $H = 500$ Oe.

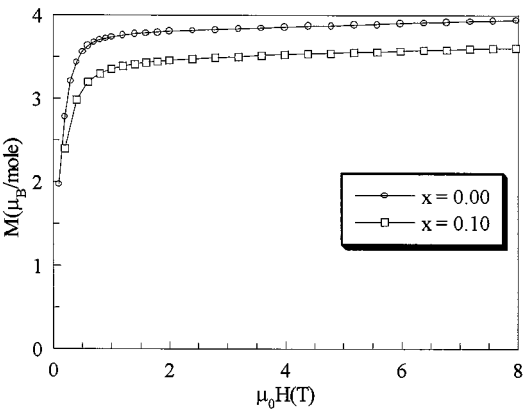

FIG. 3. Magnetization evolution as a function of magnetic applied field at $T = 4$ K for both samples $Pr_{0.7}Sr_{0.3}MnO_3$ ($x = 0$) and $Pr_{0.6}\square_{0.1}Sr_{0.3}MnO_3$ ($x = 0.1$).

The spontaneous magnetization for both samples $Pr_{0.7}Sr_{0.3}MnO_3$ and $Pr_{0.6}\square_{0.1}Sr_{0.3}MnO_3$, deduced from the magnetization evolution as a function of the magnetic applied field at $T = 4$ K (Fig. 3), is found to be 3.76 μ_B and 3.38 μ_B, respectively. These values are very closed to that obtained theoretically for full spin alignment and given by $2(\frac{4}{2} \times 0.7 + \frac{3}{2} \times 0.3) = 3.7$ μ_B for $Pr_{0.7}Sr_{0.3}MnO_3$ and $2(\frac{4}{2} \times 0.4 + \frac{3}{2} \times 0.6) = 3.4$ μ_B for $Pr_{0.6}\square_{0.1}Sr_{0.3}MnO_3$. This result confirms that our samples are not substoichiometric in oxygen.

Figure 4 shows the Curie temperature T_C evolution versus x. The Curie temperature T_C increases with increasing x from 265 K ($x = 0$) to 315 K ($x = 0.23$).

The Curie temperature T_C increase, with the Mn^{4+} content beyond 30%, is not in concordance with previous work on lanthanum- or praseodymium-substituted perovskite manganites which showed that T_C exhibits a maximum at

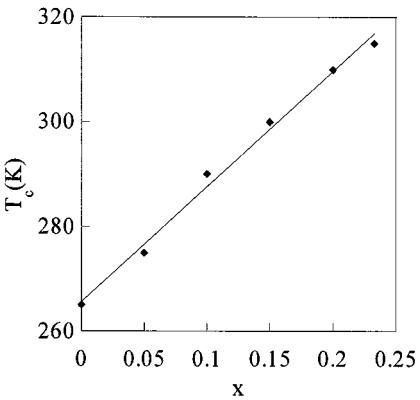

FIG. 4. Transition temperature T_C as a function of x.

about 33% Mn^{4+} content corresponding to the maximum of the double-exchange interactions (24, 25, 33). It is also not in concordance with previous work on lacunar $Pr_{0.7}Sr_{0.3-x}\square_xMnO_3$ samples where T_C was found to decrease with increasing strontium vacancy content (29). Such a result has never been observed in praseodymium perovskite manganites. Indeed, the highest T_C known to date in these compounds is about of 280 K obtained for 33% Mn^{4+} (24, 25), while our magnetic measurements show that some lacunar samples are ferromagnetic at room temperature ($T_C = 315$ K for $x = 0.23$). The ferromagnetism in these compounds with high Mn^{4+} content beyond 50% is not only governed by the Mn^{4+}/Mn^{3+} ratio; it cannot be explained only in terms of double-exchange interactions. In fact, for a given Mn^{4+} content (60%), the T_C is found to be 150 K (29) and 290 K for both lacunar $Pr_{0.7}Sr_{0.15}\square_{0.15}MnO_3$ and $Pr_{0.6}\square_{0.1}Sr_{0.3}MnO_3$ samples, respectively. Consequently, there are surely other factors which lead to such properties as the average ionic radius $\langle r_A \rangle$ effect. As a vacancy must have an average radius $\langle r_V \rangle \neq 0$, the T_C decrease with increasing strontium deficiency in the lacunar $Pr_{0.7}Sr_{0.3-x}\square_x\ MnO_3$ samples (29) and the T_C increase with increasing praseodymium deficiency in the lacunar $Pr_{0.7-x}\square_xSr_{0.3}MnO_3$ samples can be explained according to Hwang *et al.* (34) with a vacancy average radius $\langle r_V \rangle$ smaller than the radius of Sr^{2+} (1.31 Å) and larger than that of Pr^{3+} (1.179 Å).

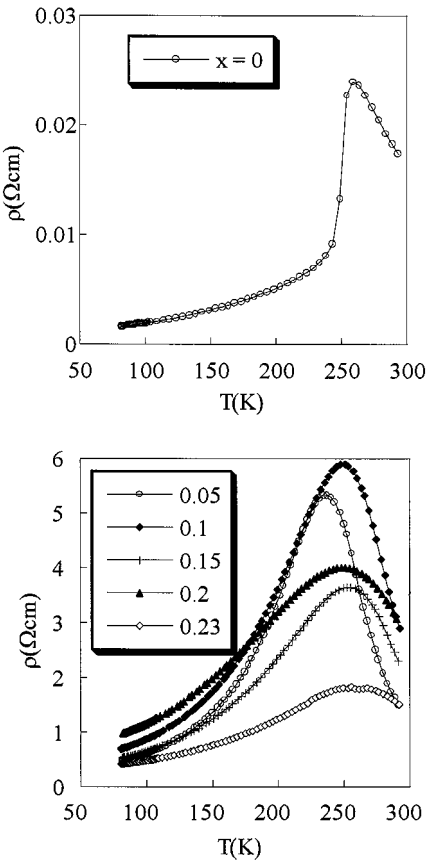

FIG. 5. Resistivity of $Pr_{0.7-x}\square_xSr_{0.3}MnO_3$ samples as a function of temperature.

3. *Electrical Properties*

Figure 5 reproduces the temperature dependence of the zero-field resistivity $\rho(T)$ in the polycrystalline samples. Using the sign of the temperature coefficient of resistivity $d\rho/dT$ as a criterion ($d\rho/dT < 0$ for a semiconductor-like system and $d\rho/dT > 0$ for a metallic system), we found that all the samples are metallic-like at low temperatures ($T < T_\rho$) and semiconductor-like above T_ρ (T_ρ corresponds to the maximum value of the resistivity).

It is important to indicate that the resistivity values of the stoichiometric sample $Pr_{0.7}Sr_{0.3}MnO_3$ are about 10^{-2} smaller than those measured in the lacunar ones. This result is in concordance with previous work on some lanthanum (35) and praseodymium (24, 25) stoichiometric manganites and also on praseodymium lacunar manganites $Pr_{0.7}Sr_{0.3-x}\square_xMnO_3$ (29), which showed an increase in the resistivity values as a function of the Mn^{4+} content above 30%.

We show in Fig. 6 the correlation between resistivity and magnetization evolutions versus temperature for various samples ($0 \leq x \leq 0.23$). These curves show a steep decrease of resistivity in accord with the onset of the ferromagnetic magnetization. Thus, the resistivity temperature dependence can be interpreted in terms of the carrier scattering by thermal spin fluctuation as well as the decrease of the hole-carrier (8–10, 36, 37). The electron (hole) transfer (t_{ij}) between the neighboring sites depends on the relative angle ($\Delta\theta_{ij}$) of the local spins in such manner as $t_{ij} = t_0 \cos(\Delta\theta_{ij}/2)$ (9). The ferromagnetic spin arrangement reduces the randomness of the transfer.

In the stoichiometric sample, the metallic–semiconducting transition occurs at the same temperature as the ferromagnetic–paramagnetic one, which indicates a strong correlation between magnetic and electrical properties. In the lacunar samples, a difference between the insulator metal and the magnetic transition temperatures has been observed. This difference becomes much larger with increasing vacancy content. This effect (the lowering of T_ρ) can be explained in terms of grain boundary effects (38) or inhomogeneity and especially for high x values.

In the ferromagnetic region, the temperature dependence of the resistivity of our samples ($0 \leq x \leq 0.23$) is described as a quadratic function of the temperature, $\rho(T) = \rho(0) + AT^2$ (Fig. 7). This result suggests an important role for the electron–electron scattering process associated with spin fluctuation. A similar result has been reported by Urushibara *et al.* (37) for $La_{1-x}Sr_xMnO_3$ single crystals and

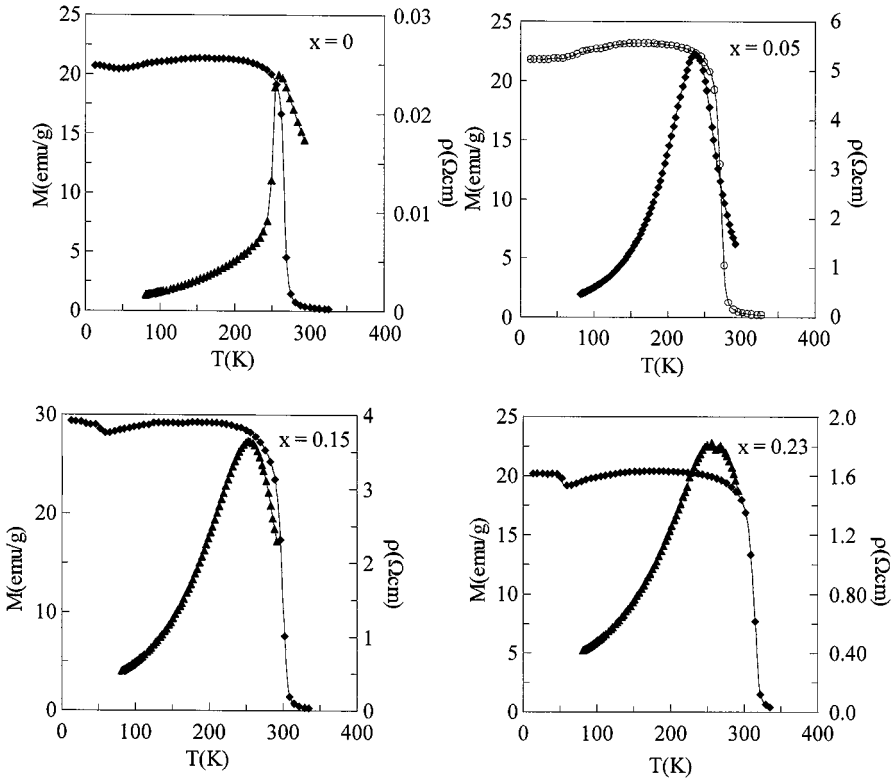

FIG. 6. Correlation between the temperature dependence of resistivity and magnetization for $Pr_{0.7-x}\square_xSr_{0.3}MnO_3$.

by Boujelben *et al.* (25) for $Pr_{1-x}Sr_xMnO_3$ polycrystalline samples.

In the semiconducting paramagnetic state ($T > T_C$), transport properties in the manganites are still a matter of controversy as numerous groups have reported different behaviors. Resistivity data can be fitted with

(i) a purely activated law $\rho = \rho_0 \exp(E_a/kT)$, where E_a is the gap energy;

(ii) a thermally activated conduction indicating hopping polaron conduction $\rho = (kT/ne^2D)\exp(E_{hop}/kT)$, where eD/kT is the Einstein diffusion mobility, n is the carrier density, D is the polaron diffusion constant, and E_{hop} is the hopping energy;

(iii) Mott's variable range hopping expression $\rho = \rho_0 \exp(T_0/T)^{1/4}$, where the Mott parameter ($T_0^{1/4}$) is proportional to the Mott localization energy.

Table 2 shows the fit results of the resistivity data in the paramagnetic state using the above laws. These results

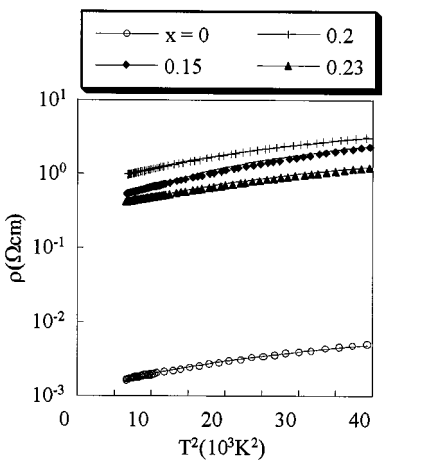

FIG. 7. Temperature dependence of the resistivity in the low-temperature region ($T < 200$ K) for $Pr_{0.7-x}\square_xSr_{0.3}MnO_3$ ($0 \le x \le 0.23$).

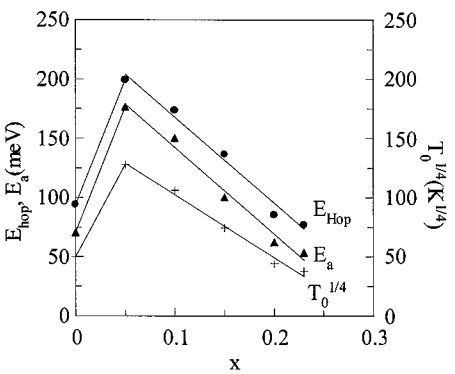

FIG. 8. Evolution of the activated energy as a function of the vacancy content.

TABLE 2
Fit Results for $Pr_{0.7-x}\square_xSr_{0.3}MnO_3$ Samples Deduced from the Three Activated Laws

	$x = 0$	$x = 0.05$	$x = 0.1$	$x = 0.15$	$x = 0.2$	$x = 0.23$
E_a (meV)	70.8	176.90	150.54	100.48	62.73	53.77
(i)	($R = 0.9996$)	($R = 0.9973$)	($R = 0.9949$)	($R = 0.9800$)	($R = 0.9815$)	($R = 0.9905$)
E_{hop} (meV)	94.2	199.34	173.73	137.18	85.88	77.15
(ii)	($R = 0.9994$)	($R = 0.9977$)	($R = 0.9960$)	($R = 0.9909$)	($R = 0.9946$)	($R = 0.9905$)
$(T_0^{1/4})$ $(K^{1/4})$	49.73	127.96	106.22	74.60	44.33	37.73
(iii)	($R = 0.9995$)	($R = 0.9983$)	($R = 0.9960$)	($R = 0.9835$)	($R = 0.9916$)	($R = 0.9829$)

show that our resistivity data can be well fit by all of them and it is really difficult to distinguish among the three laws.

We report in Fig. 8 the evolution of the activated, the hopping, and the Mott localization energy versus x. We observe an increase of the energy for $0 \leq x \leq 0.05$ followed by a decrease when x increases from 0.05 to 0.23. This decrease for $x > 0.05$ may be explained by an inhomogeneity in the samples which leads to two kinds of regions: highly defective and nearly stoichiometric. The carriers percolate through the nearly stoichiometric region, leading to an energy decrease.

IV. CONCLUSION

We have investigated the praseodymium vacancy effects on the structural, magnetic, and electrical properties of $Pr_{0.7-x}\square_xSr_{0.3}MnO_3$ powder samples. These studies show that the structural and magnetic properties are closely correlated with the vacancy content and eventually with the average cation size $\langle r_A \rangle$.

These samples crystallize in the rhombohedral structure for $x = 0$ to 0.1 and in the orthorhombic one for $x \geq 0.15$. The magnetic measurements show that these samples exhibit a ferromagnetic behavior below T_C which shifts to higher temperature from 265 K to 315 K with increasing x from 0 to 0.23. The electrical investigations show a metallic–semiconducting transition for all samples ($0 \leq x \leq 0.23$). The transition temperature T_ρ exhibits a behavior similar to that of T_C and shifts slightly to higher values with increasing praseodymium deficiency content.

REFERENCES

1. R. Von Helmolt, J. Wecker, B. Holzapfel, L. Schutz, and K. Samwer, *Phys. Rev. Lett.* **71,** 2331 (1993).
2. R. D. Sanchez, J. Rivas, C. V. Vazquez, A. L. Quintela, M. T. Causa, M. Tovar, and S. Oseroff, *Appl. Phys. Lett.* **68,** 134 (1996).
3. H. L. Ju and H. Sohn, *J. Magn. Magn. Mater.* **167,** 200 (1997).
4. W. Zhang, I. W. Boyd, N. S. Cohen, Q. T. Quentin, and A. Pankhaurst, *Appl. Surf. Sci.* **109,** 350 (1997).
5. F. Damay, C. Martin, M. Hervieu, A. Maignan, B. Raveau, G. André, and F. Bourée, *J. Magn. Magn. Mater.* **184,** 71 (1998).
6. A. Peles, H. P. Kunkel, X. Z. Zhou, and G. Williams, *J. Phys.: Condens. Matter* **11,** 8111 (1999).
7. C. Martin, A. Maignan, M. Hervieu, and B. Raveau, *Phys. Rev. B* **60,** 12191 (1999).
8. C. Zener, *Phys. Rev.* **82,** 403 (1951).
9. P. W. Anderson and H. Hasegawa, *Phys. Rev.* **100,** 675 (1955).
10. P. G. de Gennes, *Phys. Rev.* **118,** 141 (1960).
11. R. Mahesh, R. Mahendiran, A. K. Raychaudhuri, and C. N. R. Rao, *J. Solid State Chem.* **114,** 297 (1995).
12. F. Damay, C. Martin, A. Martin, and B. Raveau, *J. Appl. Phys.* **81,** 1372 (1997).
13. N. Abdelmoula, E. Dhahri, K. Guidara, and J. C. Joubert, *Phase Transitions* **69,** 215 (1999).
14. L. M. Rodriguez-Martinez and J. P. Attfield, *Phys. Rev. B* **54,** 15622 (1996).
15. F. Damay, C. Martin, A. Maignan, and B. Raveau, *J. Appl. Phys.* **82,** 6181 (1997).
16. A. K. M. Akther Hossain, L. F. Cohen, T. Kodenkandeth, J. MacManus-Driscoll, and N. M. Alford, *J. Magn. Magn. Mater.* **195,** 31 (1999).
17. I. O. Troyanchuk, S. V. Trukhanov, H. Szymezak, and K. Baerner, *J. Phys.: Condens. Matter* **12,** L155 (2000).
18. N. Abdelmoula, K. Guidara, A. Cheikh-Rouhou, E. Dhahri, and J. C. Joubert, *J. Solid State Chem.* **151,** 139 (2000).
19. A. J. Millis, P. B. Littlewood, and B. I. Shraiman, *Phys. Rev. Lett.* **74,** 5144 (1995).
20. J. Heremans, *J. Phys. D* **26,** 1149 (1993).
21. S. Jin, M. McCormack, T. H. Tiefel, and R. Ramesh, *J. Appl. Phys.* **76,** 6929 (1994).
22. K. Derbyshire and E. Korezynski, *Solid State Technol. Sept.*, 57 (1995).
23. K. Knizek, Z. Jirak, E. Pollert, F. Zounova, and S. Vratislav, *J. Solid State Chem.* **100,** 292 (1992).
24. W. Boujelben, A. Cheikh-Rouhou, M. Ellouze, and J. C. Joubert, *Phase Transitions* **71,** 127 (2000).
25. W. Boujelben, A. Cheikh-Rouhou, M. Ellouze, and J. C. Joubert, *Phys. Stat. Sol. (a)* **177,** 503 (2000).
26. L. Laroussi, J. C. Joubert, E. Dhahri, J. Pierre, and A. Cheikh-Rouhou, *Phase Transitions* (1999).
27. L. Laroussi, C. Boudaya, E. Dhahri, J. C. Joubert, and A. Cheikh-Rouhou, *Phase Transitions* **68,** 399 (1999).
28. A. Maignan, C. Michel, M. Hervieu, and B. Raveau, *Solid State Commun.* **101,** 277 (1997).
29. W. Boujelben, A. Cheikh-Rouhou, M. Ellouze, and J. C. Joubert, *Phys. Stat. Sol (a)* **181,** 451 (2000).

30. R. O. Shannon and C. T. Prewitt, *Acta Crystallogr. Sect. B* **26,** 1046 (1970).
31. B. Dabrowski, X. Xiong, Z. Bukowski, R. Dybzinski, P. W. Klamut, J. E. Siewenie, O. Chmaissem, J. Shaffer, C. W. Kimball, J. D. Jorgensen, and S. Short, *Phys. Rev. B* **60,** 7006 (1999).
32. C. Ritter, M. R. Ibarra, J. M. De Terera, P. A. Algarabel, C. Marquina, J. Blasco, J. Garcia, S. Oseroff, and S.-W. Cheong, *Phys. Rev. B* **56,** 8902 (1997).
33. G. H. Jonker, *Physica* **22,** 707 (1956).
34. H. Y. Hwang, S. W. Cheong, P. G. Radaelli, M. Marezio, and B. Batlogg, *Phys. Rev. Lett*. **75,** 914 (1995).
35. R. Von Helmolt, J. Wecker, K. Samwer, and K. Barner, *J. Magn. Magn. Mater.* **546,** 411 (1995).
36. K. Kubo and N. Ohata, *J. Phys. Soc. Jpn.* **33,** 21 (1972).
37. A. Urushibara, Y. Moritomo, T. Arima, A. Asamisu, G. Kido, and Y. Tokura, *Phys. Rev. B* **51,** 14103 (1995).
38. R. Mahendiran, R. Mahesh, A. K. Raychaudhuri, and C. N. R. Rao, *Solid State Commun.* **99,** 149 (1996).